Pergamon

0020-7225(95)00004-6

Int. J. Engng Sci. Vol. 33, No. 9, pp. 1357–1368, 1995

0020-7225/95 $9.50 + 0.00

THE INVESTIGATION OF THE INTERFACIAL CRACK BY THE OPTICAL METHOD

CHIEN-CHING MA and JANN-FANG LIN

Department of Mechanical Engineering, National Taiwan University, Taipei, Taiwan 10764, Republic of China

Abstract—The possibility of using the optical method of caustics in analysis of the interfacial crack is investigated in this study. The explicit full field solution for applying arbitrary point loadings on interfacial crack faces is used in analyzing this problem. The size of the yielding zone and the pattern of the caustics in the oscillatory and singular regions are studied by numerical simulation. The oscillatory region is found to be extremely small for most material combinations. The size of the yielding zone predicted by the Von Mises criteria is significantly larger than that of the oscillatory region. It is also very interesting to find that the patterns of the caustics inside the oscillatory region are similar to that in the singular field.

1. INTRODUCTION

In linear elastic fracture mechanics, stress intensity factors are usually used as the parameter in fracture criteria for a homogeneous body. As long as the crack tip is embedded in a homogeneous medium, the stress state around the crack tip exhibits the standard square-root singularity. For the interfacial crack, the power of stress singularity is a complex number which implies the presence of oscillations in stresses and crack surface displacements. An oscillatory singularity present in the displacements and stresses at the crack-tip for in-plane problems predicts the physically unrealistic phenomenon of interpenetration of the two materials and wrinkling of the crack faces. This zone has been indicated by Rice [1] to typically be very small under remote tensile loading, but can be large under shear loading. Many studies have been made on this subject in an effort to remove these singularities. Several modifications have been suggested for resolving this problem, such as the frictionless contact zone model of Comninou [2], the cohesive zone model of Atkinson [3] and the elastic–plastic analysis of Shih and Asaro [4]. Rice and Sih [5] analyzed the problem of a finite crack between dissimilar isotropic media and a complex stress intensity factor has been introduced by them. But the complex stress intensity factor does not have the same physical significance as those for crack in homogeneous medium. Significant progress has been recently made for a crack along an interface between dissimilar anisotropic media, which is assessed by Qu and Bassani [6], Suo [7], Wu [8] and Ma and Luo [9, 10].

The measurement of the stress intensity factor of a cracked body is the major concern in brittle fracture. Several experimental methods, such as photoelasticity, interferometry and caustic have been developed in determination of such factors. The optical shadow spot method, which is also known as the method of caustics, has been successfully applied towards the study of deformation fields in opaque solids. Advantages of caustics over other optical techniques are that the method can be applied to the investigation of both transparent or opaque materials and usage is relatively easy and it requires less equipment. The method of caustics has been initially introduced by Manogg [11] who showed that the geometrical characteristics of the caustic are dependent on the intensity of the crack tip singularity and was able to measure the intensity of the near-tip stress field. It was suggested by Rosakis and Freund [12] that the method may have potential for application in elastic–plastic fracture testing as well. In a paper of Rosakis *et al.* [13], the method of caustics for a power-law hardening material in a state of plane stress is established, a relationship between the value of Rice's J-integral and the maximum transverse diameter of the shadow spot is derived by them.

There are assumptions in deriving the method of caustics. The formula of the caustic used in

determining the stress intensity factor is therefore subjected to some restrictions. In deriving the formula of caustic, several assumptions are made, which are: (a) the specimen is in a plane stress state; (b) deformation slope is small; (c) small scale yielding prevails; (d) the measurements are made within the region of a dominant singular field. Usage of the caustic method should therefore be performed under those conditions for obtaining adequate experimental results. These assumptions have been carried through in most of the subsequent applications of caustics. Those restrictions have only been recently investigated and some conclusions have been made so as to improve the validity and accuracy of caustic method. Rosakis and Ravi-Chandar [14] analyzed the limitation of the plane stress interpretation of caustics data on compact tension specimens. The results indicated that plane-stress conditions prevail at distances from the crack tip greater than half the specimen thickness. Plasticity at the crack tip also limits the minimum distance from the tip where optical measurements can be performed. Analysis by Rosakis and Freund [15] has shown that the error introduced through the neglect of plasticity effects in the interpretation of caustics data will be small as long as the measurement is performed in a radius greater than twice the plastic zone size. The implicit assumptions of the usual small angle reflection in the evaluation of stress intensity factors by shadow spot measurements are discussed in detail by Rosakis and Zehnder [16].

The complex function of the Muskhelishvili formulations were used by Theocaris [17] to study the type and order of singularities at the interfacial crack tips by using the method of caustics. Some experimental measurements of caustics for interfacial cracks are also presented by Theocaris [17]. In his work, only the singular terms are included in the analysis of caustics in interfacial crack. Investigating the possibility of using caustic method to analyze the interfacial crack is the goal of this study. In this paper, the exact full field solutions of interfacial crack subjected to point loading at crack faces obtained by Ma and Luo [9, 10] are used for analysis of the problem. The features of the caustics for interfacial crack are investigated in detail by using the far field, singular field and oscillatory field. The yielding zone and the oscillatory region are studied and the size of the plastic region is found to be significantly larger than that of the oscillatory region. The stress fields inside and outside the oscillatory region are studied by numerical calculations. It shows that for most cases of the material combinations, the stress fields just outside the oscillatory region and along the bonded interface behave the square root singularity as those in homogeneous media.

2. FORMATION OF CAUSTICS IN REFLECTION

Consider a highly polished planar specimen of uniform thickness d in the undeformed state occupying a region in the x, y plane. When loads are applied, the equation of the deformed specimen surface is assumed to be given by $z = w(x, y) = -f(x, y)$. Consider a family of light rays parallel to the z axis, incident on the reflecting surface. Upon reflection, the light rays will deviate from parallelism. The amount of deviation for each ray is dependent on local conditions, in particular, on the local thinning of the specimen due to in-plane stresses. If certain geometrical conditions are met by the reflecting surface, then the virtual extensions of the reflected rays (dashed lines) will form an envelope of a three-dimensional surface in space as illustrated in Fig. 1. This surface, which is called the caustic surface, is the locus of points of maximum luminosity in the virtual image space. The virtual extensions of the rays are tangent to the caustic surface. The reflected light field is recorded on a camera positioned in front of the specimen. The focal plane of this camera, which will be called the "screen", is located behind the plane $z = 0$ and intersects the caustic surface at the plane $z = -z_0$, $z_0 \geq 0$. Under suitable conditions, the light field on the screen will appear as a dark spot (the shadow spot) surrounded by a bright border (the caustic curve), with diminishing light intensity away from the caustic curve. If the plane of the specimen is the x, y plane, then let the X, Y plane be the plane of the

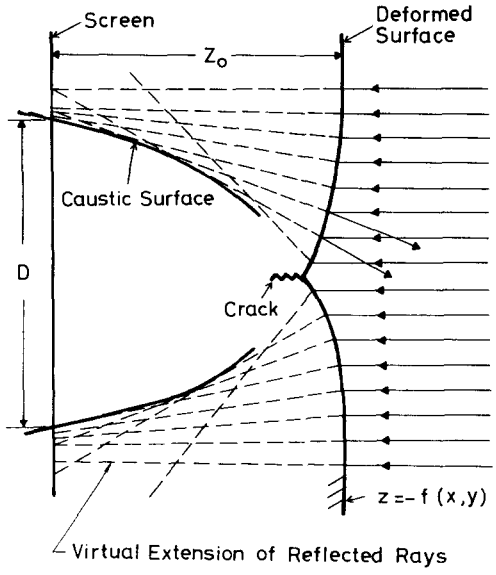

Fig. 1. Schematic diagram of optical setup for generating caustics by reflection.

screen, where the screen coordinate axes are obtained by translating the specimen coordinate axis in the directional normal to the specimen. The position of the image point on the screen is to be dependent on the slope of the reflecting surface and on the normal distance z_0, the light ray which strikes the specimen at point (x, y) then strikes the screen at the point (X, Y), the optical mapping may be written as

$$X = x - 2(z_0 - f)\frac{\partial f/\partial x}{1 - (\partial f/\partial x)^2 - (\partial f/\partial y)^2}, \tag{1a}$$

$$Y = y - 2(z_0 - f)\frac{\partial f/\partial y}{1 - (\partial f/\partial x)^2 - (\partial f/\partial y)^2}. \tag{1b}$$

If it is now assumed that $|f| \ll z_0$ and that $(\partial f/\partial x)^2 + (\partial f/\partial y)^2 \ll 1$, which is usually the case in most practical applications, the optical mapping then simplifies to

$$X = x - 2z_0\frac{\partial f}{\partial x}, \tag{2a}$$

$$Y = y - 2z_0\frac{\partial f}{\partial y}. \tag{2b}$$

Mapping equation (2) is to be used in the rest of this study. If the screen intersects with a caustic surface in the reflected light field, the resulting caustic curve on the screen then becomes a locus of points for which the mapping described by (2) is not invertable and the determinant of the Jacobian matrix of the mapping must vanish, i.e.

$$\frac{\partial(X, Y)}{\partial(x, y)} = 1 - 2z_0\left(\frac{\partial^2 f}{\partial x^2} + \frac{\partial^2 f}{\partial y^2}\right) - 4z_0^2\left[\left(\frac{\partial^2 f}{\partial x\,\partial y}\right)^2 - \frac{\partial^2 f}{\partial x^2}\frac{\partial^2 f}{\partial y^2}\right] = 0. \tag{3}$$

The points on the plane of the undeformed reflecting surface for which the Jacobian determinant vanishes are the points from which the rays forming the caustic curve are reflected. The locus of these points on the reflecting surface is the so-called initial curve. In other word, the curve on the specimen which maps into the caustic curve according to (2) is the initial curve. The light rays which strike the specimen both inside and outside of the initial curve map into points on the screen which are outside of the caustic curve. The equation of the initial curve given by equation (3) is parametrically dependent on z_0, the distance of the specimen

surface to the screen. If z_0 is small, the initial curve then becomes close to the crack tip. If z_0 is large, then the initial curve will be located far from the crack tip. Since z_0 is a variable determined by the experimental set up, the position of the initial curve can be varied at will.

Consider a plate which has a uniform thickness of d in the undeformed state. If the plate is subjected to loading, the resulting change is thickness in terms of the in-plane stress components which is given by

$$f(x, y) = -w(x, y) = \frac{\nu d}{2E}(\sigma_{xx} + \sigma_{yy}), \tag{4}$$

where ν is the Poisson's ratio; E is the elastic modulus; and w is the displacement in the thickness direction. In terms of the stress distribution, the mapping equations (2) become

$$X = x - \frac{z_0 \nu d}{E}\frac{\partial(\sigma_{xx} + \sigma_{yy})}{\partial x}, \tag{5a}$$

$$Y = y - \frac{z_0 \nu d}{E}\frac{\partial(\sigma_{xx} + \sigma_{yy})}{\partial y}. \tag{5b}$$

3. CAUSTICS FOR INTERFACIAL CRACKS

The analytical full field solutions of stresses for isotropic interfacial crack are obtained on the basis of the results from Ma and Luo [9]. We consider two arbitrary point loadings applied on the semi-infinite crack faces with distance a from the crack tip as shown in Fig. 2. Perfect bonding along the interface is ensured by the stress and displacement continuity conditions. The deformation field $f(x, y)$ expressed in (4) depends only on the invariance of stress $\sigma_{xx} + \sigma_{yy}$. The problem is solved by application of the Mellin transform in conjunction with the complex stress function and the full field analytical solutions are obtained explicitly. Among the publications on problems involving cracks in dissimilar isotropic media, those of particular interest are by England [18], Erdogen [19] and Rice and Sih [5]. Most of the papers on interfacial crack problem have focused attention on the oscillatory region. With the complete solutions in hand, we are able to investigate the interfacial crack in more detail. The stress invariance in the upper material can be expressed as follows

$$\begin{aligned}\mathbf{I}_1 &= \sigma_{xx} + \sigma_{yy} \\ &= \frac{(\underline{\mathscr{G}}\mathscr{V})_{\beta^2=1}}{\pi(\eta + \xi + \eta^* + \xi^*)(a + z)} + \frac{(\bar{\underline{\mathscr{G}}}\mathscr{V})_{\beta^2=1}}{\pi(\eta + \xi + \eta^* + \xi^*)(a + \bar{z})} \\ &\quad + \frac{(\underline{\mathscr{G}}\mathscr{V})_{\beta^2=-e^{2\pi\beta}}}{\pi i e^{\pi\beta}(1 + e^{2\pi\beta})(-2\ell e^{2\pi\beta} + m)(a + z)}\left(\frac{z}{a}\right)^{-1/2-i\beta} \\ &\quad + \frac{(\bar{\underline{\mathscr{G}}}\mathscr{V})_{\beta^2=-e^{2\pi\beta}}}{-\pi i e^{\pi\beta}(1 + e^{2\pi\beta})(-2\ell e^{2\pi\beta} + m)(a + \bar{z})}\left(\frac{\bar{z}}{a}\right)^{-1/2+i\beta}\end{aligned}$$

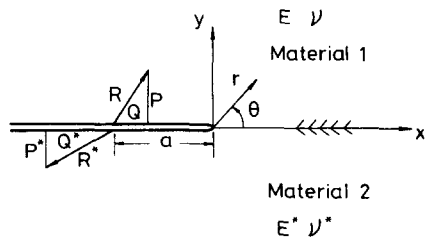

Fig. 2. Bonded isotropic dissimilar interfacial crack.

$$+\frac{(\underline{\mathscr{G}}\mathscr{V})_{\hbar^2=-e^{-2\pi\beta}}}{\pi i e^{-\pi\beta}(1+e^{-2\pi\beta})(-2\ell e^{-2\pi\beta}+m)(a+z)}\left(\frac{z}{a}\right)^{-1/2-i\beta}$$

$$+\frac{(\bar{\underline{\mathscr{G}}}\mathscr{V})_{\hbar^2=-e^{-2\pi\beta}}}{-\pi i e^{-\pi\beta}(1+e^{-2\pi\beta})(-2\ell e^{-2\pi\beta}+m)(a+\bar{z})}\left(\frac{\bar{z}}{a}\right)^{-1/2+i\beta}, \tag{6}$$

where

$$\hbar = e^{-i(s+1)\pi},$$

$$\underline{\mathscr{G}} = R[\xi - \xi^* - (\xi + \eta^*)\hbar^2] - R^*(\eta^* + \xi^*),$$

$$\mathscr{V} = -[\xi + \eta^* + (\eta + \xi^*)\hbar^2],$$

$$\eta = (\psi - 1)/\mu, \qquad \xi = 1/\mu,$$

$$\eta^* = (\psi^* - 1)/\mu^*, \qquad \xi^* = 1/\mu^*,$$

$$\psi = 4/(1+\nu) \qquad \text{for plane stress,}$$

$$\psi = 4(1-\nu) \qquad \text{for plane strain,}$$

$$\ell = -(\eta + \xi^*)(\xi + \eta^*),$$

$$m = -(\eta + \xi^*)^2 - (\xi + \eta^*)^2,$$

$$z = x + iy,$$

in which μ is the shear modulus and ν is the Poisson ratio. The overbar means the complex conjugate and the variable with superscript symbol $*$ means the material constant in the lower plane. It is worthy to note that ξ, η, ξ^* and η^* are real values, so are ℓ and m. The solution of the stress invariance in the lower half plane can be obtained by replacing $\underline{\mathscr{G}}$ and $\bar{\underline{\mathscr{G}}}$ to $\underline{\mathscr{G}}^*$ and $\bar{\underline{\mathscr{G}}}^*$, respectively, in which

$$\underline{\mathscr{G}}^* = -R^*[\eta + \xi^* + (\xi - \xi^*)\hbar^2] - R(\eta + \xi)\hbar^2.$$

The complex constant $R = Q + iP$ is denoted as the applied point loading on the upper crack face as shown in Fig. 2 and $R^* = -Q^* - iP^*$. We can see very clearly that the singular field comes from the last four terms in (6). The expression for the invariance of stress $\sigma_{xx} + \sigma_{yy}$ in the singular field as $r \to 0$ can be approximated by

$$\lim_{r\to 0} \mathbf{I}_1 = \lim_{r\to 0} \sigma_{xx} + \sigma_{yy}$$

$$= \frac{(\underline{\mathscr{G}}\mathscr{V})_{\hbar^2=-e^{2\pi\beta}}}{\pi a i e^{\pi\beta}(1+e^{2\pi\beta})(-2\ell e^{2\pi\beta}+m)}\left(\frac{z}{a}\right)^{-1/2-i\beta}$$

$$+\frac{(\bar{\underline{\mathscr{G}}}\mathscr{V})_{\hbar^2=-e^{2\pi\beta}}}{-\pi a i e^{\pi\beta}(1+e^{2\pi\beta})(-2\ell e^{2\pi\beta}+m)}\left(\frac{\bar{z}}{a}\right)^{-1/2+i\beta}$$

$$+\frac{(\underline{\mathscr{G}}\mathscr{V})_{\hbar^2=-e^{-2\pi\beta}}}{\pi a i e^{-\pi\beta}(1+e^{-2\pi\beta})(-2\ell e^{-2\pi\beta}+m)}\left(\frac{z}{a}\right)^{-1/2-i\beta}$$

$$+\frac{(\bar{\underline{\mathscr{G}}}\mathscr{V})_{\hbar^2=-e^{-2\pi\beta}}}{-\pi a i e^{-\pi\beta}(1+e^{-2\pi\beta})(-2\ell e^{-2\pi\beta}+m)}\left(\frac{\bar{z}}{a}\right)^{-1/2+i\beta}. \tag{7}$$

The order of the stress singularity $\lambda = -\frac{1}{2} - i\beta$ (or $\lambda = -\frac{1}{2} + i\beta$) is a complex number and the

stress fields are oscillatory in the limit $r \to 0$. The magnitude of the oscillation depends on the value β which can be expressed as

$$\beta = \frac{1}{\pi}\tanh^{-1}\left[\frac{\mu^*(\psi - 2) - \mu(\psi^* - 2)}{\mu\psi^* + \mu^*\psi}\right].$$

The value of β is a nondimensional real number measuring an aspect of the dissimilarity of the two materials and is referred to as the oscillatory index. The maximum value of β is found to be $(\ln\sqrt{3})/\pi(\approx 0.175)$. The combination of material constants that make no oscillation in the stress fields will be $\beta = 0$, or the condition that $\mu^*(\psi - 2) = \mu(\psi^* - 2)$. Homogeneous materials obviously satisfy this condition. The mapping equation by using the full field solution becomes

$$\begin{aligned}
X = x - \frac{z_0 vd}{E}\Bigg\{ & \frac{(\underline{\mathscr{G}}\mathscr{V})_{|\ell|^2=1}}{\pi(\eta + \xi + \eta^* + \xi^*)(a+z)^2} + \frac{(\underline{\bar{\mathscr{G}}}\mathscr{V})_{|\ell|^2=1}}{\pi(\eta + \xi + \eta^* + \xi^*)(a+\bar{z})^2} \\
& - \frac{(\underline{\mathscr{G}}\mathscr{V})_{|\ell|^2=-e^{2\pi\beta}}}{\pi e^{\pi\beta}(1+e^{2\pi\beta})(-2\ell e^{2\pi\beta} + m)(2a)(a+z)^2} \\
& \times \left(\frac{z}{a}\right)^{-3/2-i\beta} [2(a+z)\beta - (a+3z)i] \\
& - \frac{(\underline{\bar{\mathscr{G}}}\mathscr{V})_{|\ell|^2=-e^{2\pi\beta}}}{\pi e^{\pi\beta}(1+e^{2\pi\beta})(-2\ell e^{2\pi\beta} + m)(2a)(a+\bar{z})^2} \\
& \times \left(\frac{\bar{z}}{a}\right)^{-3/2+i\beta} [2(a+\bar{z})\beta + (a+3\bar{z})i] \\
& - \frac{(\underline{\mathscr{G}}\mathscr{V})_{|\ell|^2=-e^{-2\pi\beta}}}{\pi e^{-\pi\beta}(1+e^{-2\pi\beta})(-2\ell e^{-2\pi\beta} + m)(2a)(a+z)^2} \\
& \times \left(\frac{z}{a}\right)^{-3/2-i\beta} [-2(a+z)\beta - (a+3z)i] \\
& - \frac{(\underline{\bar{\mathscr{G}}}\mathscr{V})_{|\ell|^2=-e^{-2\pi\beta}}}{\pi e^{-\pi\beta}(1+e^{-2\pi\beta})(-2\ell e^{-2\pi\beta} + m)(2a)(a+\bar{z})^2} \\
& \times \left(\frac{\bar{z}}{a}\right)^{-3/2+i\beta} [-2(a+\bar{z})\beta + (a+3\bar{z})i]\Bigg\},
\end{aligned} \tag{8}$$

$$\begin{aligned}
Y = y - \frac{z_0 vd}{E}\Bigg\{ & \frac{(\underline{\mathscr{G}}\mathscr{V})_{|\ell|^2=1}}{\pi(\eta + \xi + \eta^* + \xi^*)(a+z)^2} + \frac{(\underline{\bar{\mathscr{G}}}\mathscr{V})_{|\ell|^2=1}}{\pi(\eta + \xi + \eta^* + \xi^*)(a+\bar{z})^2} \\
& - \frac{(\underline{\mathscr{G}}\mathscr{V})_{|\ell|^2=-e^{2\pi\beta}}}{\pi e^{\pi\beta}(1+e^{2\pi\beta})(-2\ell e^{2\pi\beta} + m)(2a)(a+z)^2} \\
& \times \left(\frac{z}{a}\right)^{-3/2-i\beta} [(a+3z) + 2(a+z)\beta i] \\
& - \frac{(\underline{\bar{\mathscr{G}}}\mathscr{V})_{|\ell|^2=-e^{2\pi\beta}}}{\pi e^{\pi\beta}(1+e^{2\pi\beta})(-2\ell e^{2\pi\beta} + m)(2a)(a+\bar{z})^2} \\
& \times \left(\frac{\bar{z}}{a}\right)^{-3/2+i\beta} [(a+3\bar{z}) - 2(a+\bar{z})\beta i] \\
& - \frac{(\underline{\mathscr{G}}\mathscr{V})_{|\ell|^2=-e^{-2\pi\beta}}}{\pi e^{-\pi\beta}(1+e^{-2\pi\beta})(-2\ell e^{-2\pi\beta} + m)(2a)(a+z)^2}
\end{aligned}$$

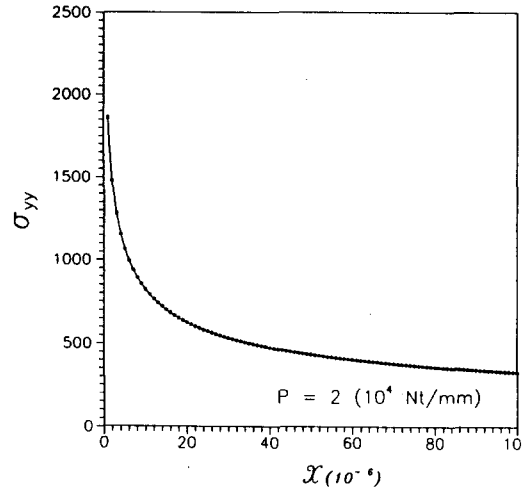

Fig. 3. The stress σ_{yy} in the singular field along the interface.

$$\times\left(\frac{z}{a}\right)^{-3/2-i\beta}[(a+3z)-2(a+z)\beta i]$$

$$-\frac{(\bar{\mathcal{G}}\mathcal{V})_{i^2=-e^{-2\pi\beta}}}{\pi e^{-\pi\beta}(1+e^{-2\pi\beta})(-2\ell e^{-2\pi\beta}+m)(2a)(a+\bar{z})^2}$$

$$+\left(\frac{\bar{z}}{a}\right)^{-3/2+i\beta}[(a+3\bar{z})+2(a+\bar{z})\beta i]\Big\}. \tag{9}$$

In linear elastic fracture mechanics, stress intensity factors are usually used as the parameter in fracture criteria for homogeneous body. As long as the crack tip is embedded in a homogeneous medium, the stress state around the crack tip exhibits the standard square root singularity. For the interfacial crack, the stresses share the inverse square root singularity of the crack and, in addition, exhibit an oscillatory behavior as the crack tip is approached. Due to the presence of the oscillatory complex types of singularities for the interfacial crack problems. The classical definition of the stress intensity factor in homogeneous materials can not be used in this case. Some researchers are made to study the definition of the stress intensity factor in interfacial crack, e.g. Rice and Sih [5], Hutchinson *et al.* [20], Rice [21], Wu [8] and Suo [7]. A more detailed investigation on the near tip region will be reported in the next section.

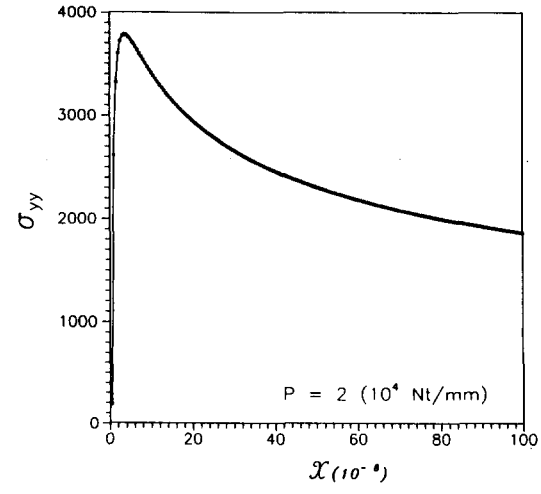

Fig. 4. The stress σ_{yy} in the oscillatory field along the interface.

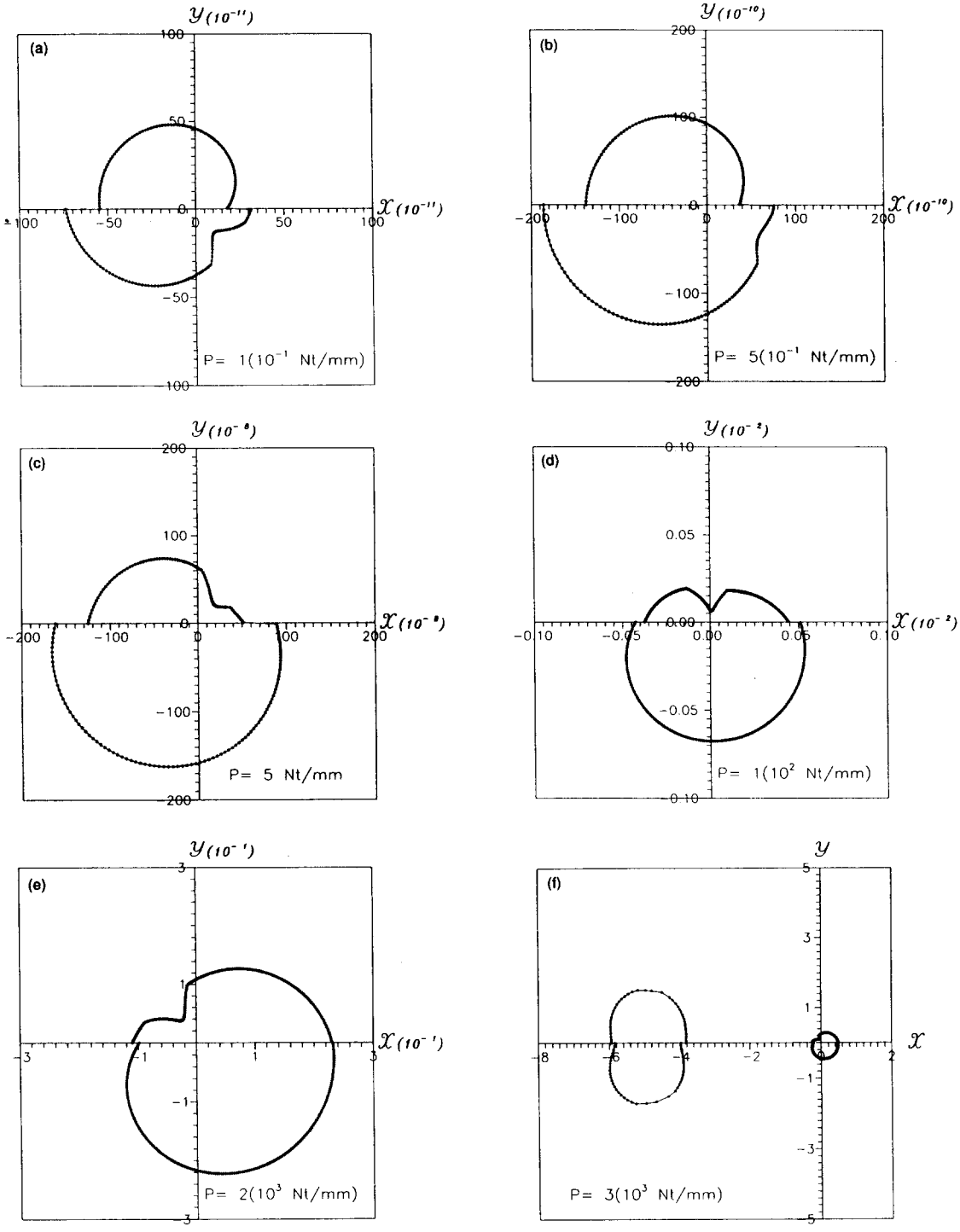

Fig. 5. *Continued opposite.*

4. NUMERICAL SIMULATIONS

The yielding zone, the caustics inside the oscillatory region and singular field are investigated in this section by numerical simulations. The material constants chosen for the numerical investigation are $\mu = 5$ GPa, $\nu = 0.3$, $\mu^* = 1$ GPa and $\nu^* = 0.3$. This material combination will make the oscillatory index $\beta = 0.075$. The maximum value of β is found to be $\ln\sqrt{3}/\pi(\approx 0.175)$. The value of β is normally quite small (usually under 0.05) for most material combinations. The

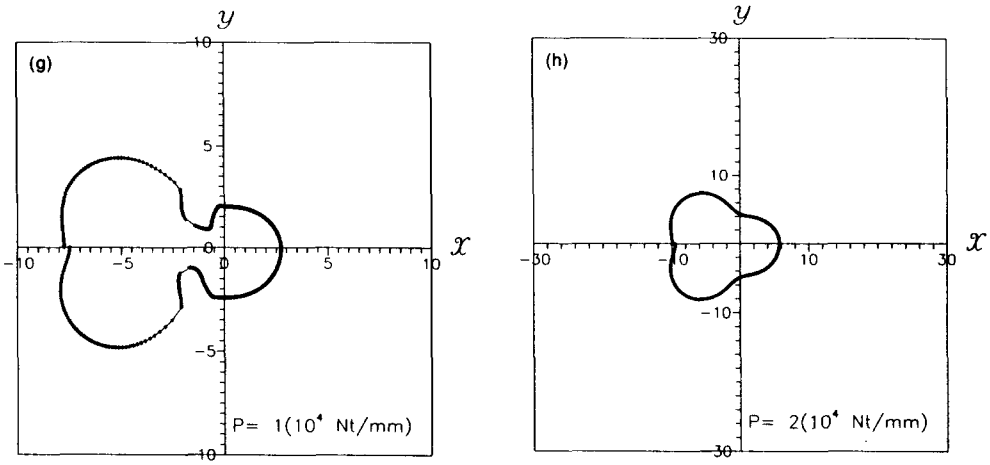

Fig. 5. The yielding zone for applying point loading with the magnitude (a) $P = 10^{-1}$ Nt/mm; (b) $P = 5 \times 10^{-1}$ Nt/mm; (c) $P = 5$ Nt/mm; (d) $P = 10^2$ Nt/mm; (e) $P = 2 \times 10^3$ Nt/mm; (f) $P = 3 \times 10^3$ Nt/mm; (g) $P = 10^4$ Nt/mm; (h) $P = 2 \times 10^4$ Nt/mm.

magnitude of β is dependent only on material constants and is independent on the applied loading. The distance from the symmetrical applied loads ($Q = Q^* = 0$) is set to 5 mm. Figure 3 shows the singular field of σ_{yy} along the interface for x is small. The oscillation of stress is found in Fig. 4 begin in the order of 10^{-8} mm. The oscillatory region is dependent on β and is extremely small which is in the order of one-tenth of the atomic dimension. Hence the linear elasticity and continuum theory are not applicable in this region practically. The size and shape of the yielding zone for the interfacial crack are predicted by the Von Mises criteria and the results are plotted in Fig. 5. The yielding stress in the upper material is assumed to be 0.8 and 0.6 GPa for lower material. These figures show the shape and the size change of the yielding

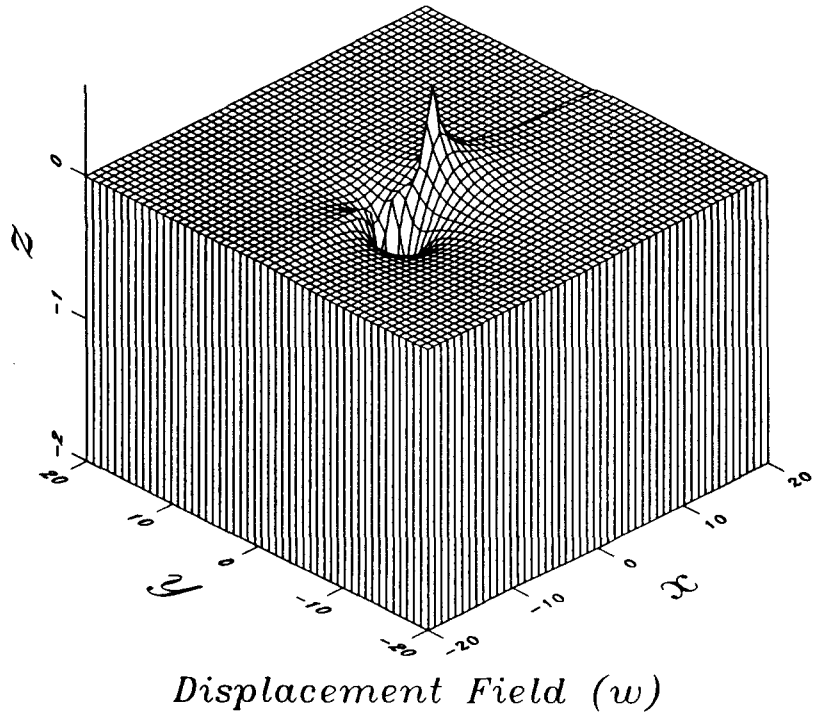

Fig. 6. The displacement field near the interfacial crack tip.

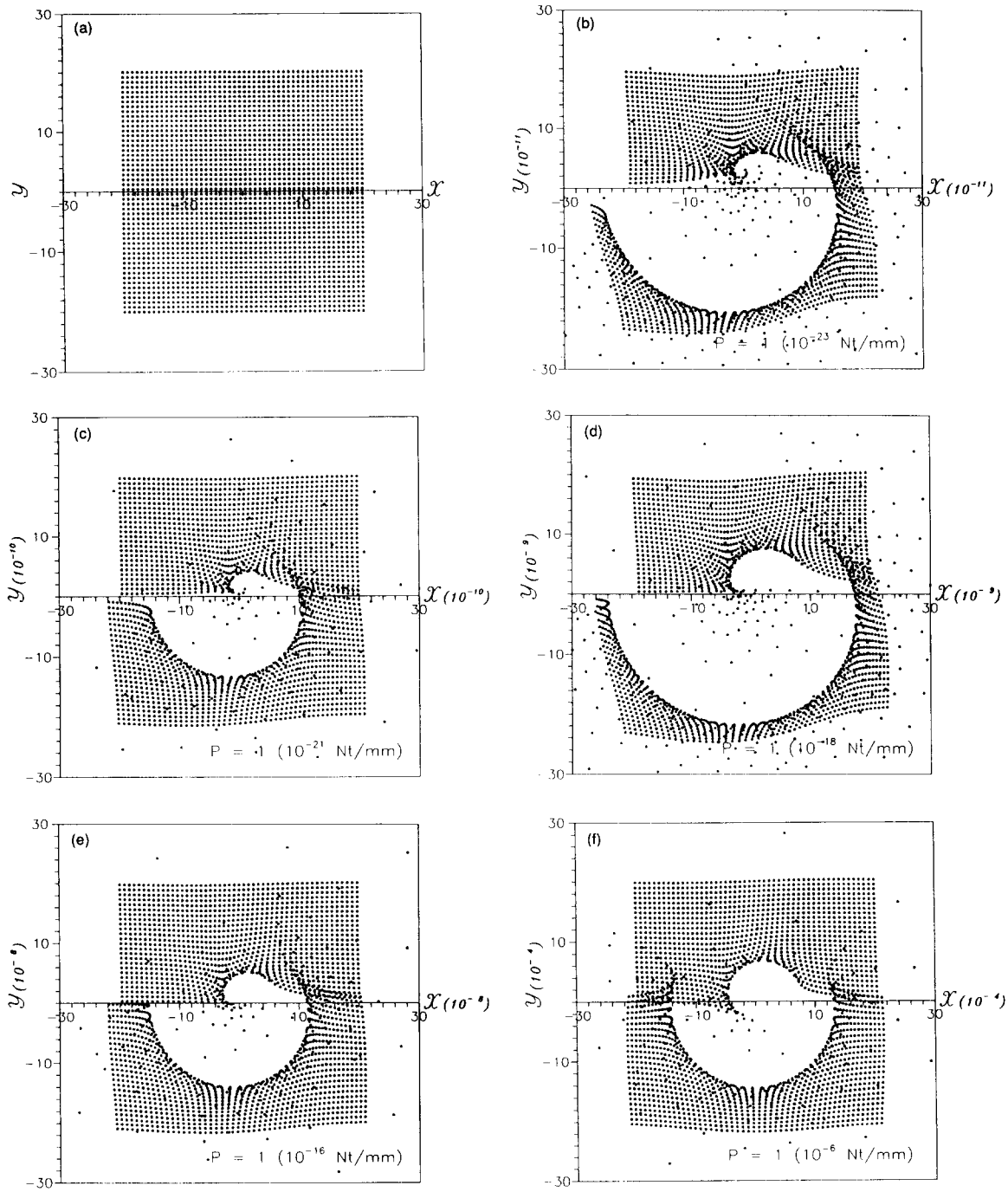

Fig. 7. *Continued opposite.*

zone for the region inside the oscillatory zone to the full field solution as the applied load increases. Two separate regions of the plastic zone shown in Fig. 5(f) exhibit here that one region is near the crack tip and the other one is near the applied concentrated load. Figures 5(g) and (h) show the linkage of these two plastic regions when the applied load is large enough. The size of the plastic zone is shown in Fig. 5 to usually be larger than that of the oscillatory region near the interfacial crack tip.

The displacement field near the interfacial crack is plotted in Fig. 6. In order to fully understand the phenomenon of caustic formation of an interfacial crack, the reflected optical field is simulated numerically. In order to understand the character of the caustic inside the

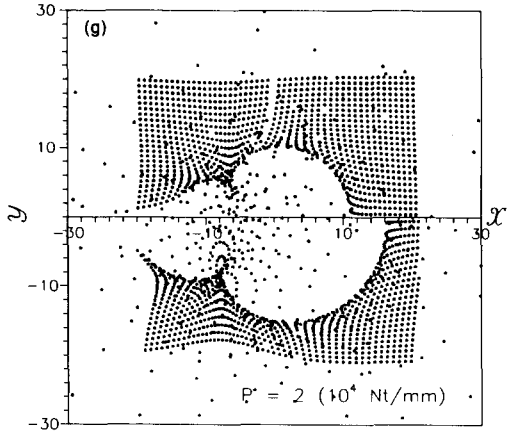

Fig. 7. (a) Regular array of incident light rays. The caustic pattern for applying point loading with the magnitude (b) $P = 10^{-23}$ Nt/mm; (c) $P = 10^{-21}$ Nt/mm; (d) $P = 10^{-18}$ Nt/mm; (e) $P = 10^{-16}$ Nt/mm; (f) $P = 10^{-6}$ Nt/mm; (g) $P = 2 \times 10^{4}$ Nt/mm.

oscillatory region, we assume that the oscillatory region does exist and the continuum theory can be applied. In this study, a square array of light rays was assumed to be normally incident on the surface of the specimen. The pattern in which these light rays pierce the plane reflecting surface of the undeformed specimen is shown in Fig. 7(a). These light rays were then reflected from a surface deformed according to (8) and (9). The patterns of reflected rays that would be observed on the screen are shown in Fig. 7 for the region of the oscillatory field, the singular field and the full field. In these figures, the value of z_0 is chosen to be 500 mm for numerical calculations. It is seen in these figures that the caustics inside the oscillatory region are similar to that in the singular field.

The stress field just outside the oscillatory region will be discussed for the oscillatory index $\beta = 0.075$. The predicted oscillatory zone is confined to a distance that is smaller than physically relevant length scales as pointed out previously. Hence we can consider this oscillatory region as the nonlinear zone just like the plastic zone or process zone. If this oscillatory region is extremely small and outside this region there does indeed exist an ordinary stress intensity factor field, then the classical concept for stress intensity factor in homogeneous body may be applied for the interfacial crack problems as well. In Fig. 8, the solid line represents the exact solution of stress along the crack tip line and the dashed line indicates K field with square root singularity from the ordinary definition. This figure shows that immediately outside the oscillatory region, the stress behaves square root singularity just like the homogeneous crack.

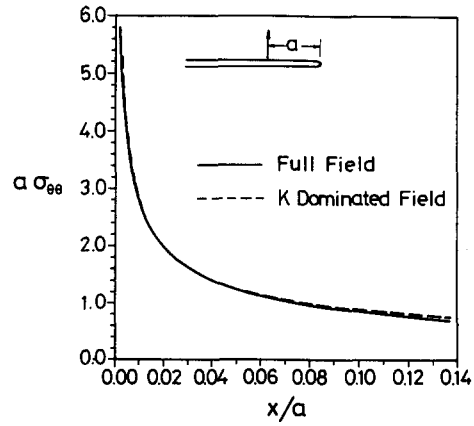

Fig. 8. The comparison of the solution of the stress immediately outside the oscillatory region and the K dominate field.

Hence, the use of the classical definition of the stress intensity factor in homogeneous material as a possible fracture parameter in interfacial crack may be a worthy direction of research.

5. CONCLUSIONS

Many engineering structures are comprised of more than one material and interfacial crack occurs frequently along the interface. All the analytical studies of inplane interfacial crack have shown that the stresses share the inverse square root singularity of the crack and, in addition, exhibit an oscillatory behavior as the crack tip is approached. A physically unrealistic phenomenon is inferred to occur by this oscillatory behavior. For most cases of different material combinations, the imaginary part of the stress singularity is extremely small which indicates that the oscillatory region is rather small as compared to other physical dimensions. The problem of interfacial crack has been investigated in this study in more detail. Since the oscillatory region is independent to the applied loading, the yield zone has been found to be larger than the oscillatory region for most cases of applied loadings in practical. It is also very interesting to see that caustic patterns inside the oscillatory region are quite similar to that in the singular region.

As indicated previously in this study that the oscillatory region is confined to a distance that is smaller than physically relevant length scales. Furthermore the plastic zone developed near the crack tip is larger than the physically unrealistic oscillatory region. This small region can therefore be considered here as the nonlinear zone or the process zone. It is also indicated in this study that immediately outside the oscillatory region of the interfacial crack, the stress behaves square root singularity just like the crack in homogeneous medium. Based on this founding, it seems possible that the classical definition of stress intensity factor for the square root singularity can also be applied in the interfacial crack problem as well. Usage of the stress intensity factor as a possible fracture parameter in the interfacial crack problem may therefore be a worthy direction of future research. A further study on the investigation for the measurement of fracture parameters related to the caustic method will be given in a follow-up report.

Acknowledgement—The financial support by the National Science Council (Republic of China) through grant NSC 80-0401-E002-29 to the National Taiwan University is gratefully acknowledged.

REFERENCES

[1] J. R. RICE, *J. Appl. Mech.* **55,** 98 (1988).
[2] M. COMNINOU, *J. Appl. Mech.* **44,** 631 (1977).
[3] C. ATKINSON, *Int. J. Fracture* **13,** 807 (1977).
[4] C. F. SHIH and R. J. ASARO, *J. Appl. Mech.* **55,** 299 (1988).
[5] J. R. RICE and G. C. SIH, *J. Appl. Mechanics* **32,** 418 (1965).
[6] J. QU and J. L. BASSANI, *J. Mech. Phys. Solids* **37,** 417 (1989).
[7] Z. SUO, *Proc. R. Soc. Lond.* **A427,** 331 (1990).
[8] K. C. WU, *J. Appl. Mechanics* **57,** 882 (1990).
[9] C. C. MA and J. J. LUO, Accepted for publication in *J. Engng Mech.*
[10] C. C. MA and J. J. LUO, *J. Appl. Mechanics* **60,** 777 (1993).
[11] P. MANOGG, Anwendungen der Schattenoptik zur Untersuchung des Zerreissvorgags von Platten. Doctoral dissertation, University of Freiburg (1964).
[12] A. J. ROSAKIS and L. B. FREUND, *J. Engng Mater. Technol.* **104,** 115 (1982).
[13] A. J. ROSAKIS, C. C. MA and L. B. FREUND, *J. Appl. Mechanics* **50,** 777 (1983).
[14] A. J. ROSAKIS and K. RAVI-CHANDAR, *Int. J. Solids Structures* **22,** 121 (1986).
[15] A. J. ROSAKIS and L. B. FREUND, *J. Appl. Mechanics* **48,** 302 (1981).
[16] A. J. ROSAKIS and A. T. ZEHNDER, *J. Elasticity* **15,** 347 (1985).
[17] P. S. THEOCARIS, *Acta Mechanica* **24,** 99 (1976).
[18] A. H. ENGLAND, *J. Appl. Mechanics* **32,** 400 (1965).
[19] F. ERDOGAN, *J. Appl. Mechanics* **32,** 403 (1965).
[20] J. W. HUTCHINSON. M. E. MEAR and J. R. RICE, *J. Appl. Mechanics* **54,** 828 (1987).
[21] J. R. RICE, *J. Appl. Mechanics* **55,** 98 (1988).

(Revision received 25 April 1994; accepted 28 December 1994)